Analysis and design of plasmon systems for telecom applications

Andres Barbosa Neira

Thesis director:

Olivier Martin

Ecole Polytechnique Federale de Lausanne

Laboratory of Nanophotonics and Metrology

Lausanne-Switzerland

2010

ABSTRACT

Analysis of both surface plasmon polariton and localized plasmon is performed. Through simulations realized in MATLAB, their theory is analyzed. After that, using the previous results plasmon systems like plasmon waveguides and nanoantennae are also analyzed. For plasmon waveguides, losses and mode profiles are calculated and simulated at telecom wavelengths (1.55μm) using COMSOL, followed by a comparison of different kind of plasmon waveguides known in the literature. For nanoantennae, their dimensions are designed for resonate at 1.55μm, using simulations applying the green's tensor method. For its excitement, the evanescent field of a guided mode in a planar waveguide is used. An experimental setup is also designed for the measurement of the nanoantennae radiation produced by this excitation. Results from the plasmon waveguide analysis show some outlines in the design of plasmon waveguides according to the bending and the propagation distance. In the case of the nanoantennae there are still some improvements to be made in the excitation method and in their design.

Keywords: nanoantennae, plasmon, waveguide, telecom, wavelength, MATLAB, COMSOL, resonance, losses, polarization.

INTRODUCTION

Plasmons are the quanta of Plasma oscillation. As photons and phonons are the quanta for light and heat oscillations, plasmons are collective oscillations of the free electron gas that may exist in metals at optical frequencies. There are three different kinds of plasmon. In this work we are going to treat two of them, because those are the most useful for practical applications.

The non-localized plasmon or surface plasmon polaritons (SPP) is an electromagnetic wave that propagates in the surface of a metallic material. Due to the interaction between the photons and electrons in this kind of surfaces, the SPP can be greatly confined in regions under the diffraction limit. This characteristic makes them one of the most reliable alternative for integrating photonic circuits (like waveguides, ring oscillators, interferometers, etc), with electronic circuits [1]. One consequence of this integration is that you can transform the electrical signal into an optical signal and then transmit it to another part in the chip, using optical interconnections which are faster than electrical interconnections (the speed limit only depends of the speed of light in the media), so in this way you can go above of the speed limit imposed by actual electronic devices and achieved a higher performance [2].

The localized plasmons are plasmon resonances which occur in systems which dimensions are very small in comparison with the wavelength. This resonance cause an enhancement of the field in very small regions, which has a lot of applications in biology for enhancing the fluorescence signal for single-molecule detection, or in photovoltaic for increasing the efficiency of solar panels [3][4][5].

In this work we are going to do a deep study in the behavior of plasmons, and we will analyze different kinds of plasmon systems in order to have some outlines in their design. We are going to start from the beginning, by analyzing the theory of them. Then we are going to analyze the surface and localized plasmons. We are going to perform simulations to analyze both of them, and for the case of localized plasmons, we are going to fabricate a plasmonic system and then realize and experimental setup for its measurement.

ELECTROMAGNETISM OF METALLIC MATERIALS

The behavior of metals and more precisely of the conductivity of metals varies according to the frequency. This behavior has never taken into account because metals were always used in frequencies under the optical regime, where they actually are very refractive and don't allow electromagnetic waves to propagate inside of them. But in the optical regime they result to be very absorptive, increasing the losses of any photonic system when scaled down. In fact, when going in the ultraviolet regime, some of them became transparent and even allow electromagnetic waves to propagate inside of them. This is the case for example of the sodium.

Using Maxwell equations, it is possible to show that there is an equation which relates the conductivity of a metal with the dielectric relative permittivity of the metal. This equation is

$$\varepsilon = 1 + i\frac{\sigma}{\varepsilon_0 \omega}$$

And if we say that the conductivity has dependence in the frequency we can write this equation like

$$\varepsilon(\omega) = 1 + i\frac{\sigma(\omega)}{\varepsilon_0 \omega} \quad (1)$$

The Plasma Model

Over a large range, the plasma model (also called drude model) explains very good the optical properties of metals. In this model, the gas of free electrons of density n, inside the metal moves against a background of positive ion cores. This model works very good for alkali metals even in the ultraviolet range. But for noble metals, like gold, interband transitions occur at visible frequencies which reduce the validity of this model.

In this model, details in the lattice potential and in the electron-electron interaction are not calculated precisely. Instead, in order to take into account for these details we add a certain value of effective mass m for the lattice potential, and a certain damping $\gamma = 1/\tau$ for the collisions between electrons. In the previous relation, τ is known as the relaxation time of the gas of free electrons and it is in the order of 10^{-14} s.

According to this model, the equation for the motion of free elects gas is:

$$m\ddot{\vec{x}} + m\gamma\dot{\vec{x}} = -e\vec{E}$$

Assuming that we have an harmonic time dependence for the electric field, we can assume a solution for x in the form $x(t) = x_0 e^{-i\omega t}$. Solving the equation for this kind of solution we find out

$$\overrightarrow{\boldsymbol{x}(\boldsymbol{t})} = \frac{ne^2}{m(\omega^2 + i\gamma\omega)}\overrightarrow{\boldsymbol{E}(\boldsymbol{t})}$$

Using $\vec{P} = -ne\overrightarrow{\boldsymbol{x}(\boldsymbol{t})}$, which relates the total polarization generated by the electrons gas and then inserting the polarization in the relation between electric field and displacement field, we can find out that the dependence in the frequency of the permittivity is:

$$\varepsilon(\omega) = 1 - \frac{{\omega_p}^2}{\omega^2 + i\gamma\omega} \quad (2)$$

For frequencies close to ω_p, the damping of the system can be considered negligible so the last equation becomes

$$\varepsilon(\omega) = 1 - \frac{{\omega_p}^2}{\omega^2} \quad (3)$$

Here $\omega_p = \frac{ne^2}{\varepsilon_0 m}$ is known as the *plasma frequency* of the free electron gas. To understand its meaning we have to first take into consideration the wave equation which in the Fourier domain is:

$$\vec{\boldsymbol{k}} \times \left(\vec{\boldsymbol{k}} \times \vec{\boldsymbol{E}}\right) = -\varepsilon(\omega)\frac{\omega^2}{c^2}\vec{\boldsymbol{E}} \;\; or \;\; \vec{\boldsymbol{k}}\left(\vec{\boldsymbol{k}} \cdot \vec{\boldsymbol{E}}\right) - \; k^2\vec{\boldsymbol{E}} = -\varepsilon(\omega)\frac{\omega^2}{c^2}\vec{\boldsymbol{E}}$$

For transversal waves we have the condition $\vec{\boldsymbol{k}} \cdot \vec{\boldsymbol{E}} = 0$ which leads to:

$$k^2 = \varepsilon(\omega)\frac{\omega^2}{c^2}$$

And for longitudinal waves we have the condition $\vec{\boldsymbol{k}} \times \vec{\boldsymbol{E}} = 0$ which leads to

$$\varepsilon(\omega) = 0$$

From (3) we can see that this condition can only be fulfilled at the plasma frequency, which means that at the plasma frequency, we will have longitudinal waves of the free electron gas.

Different kinds of plasmon

There are three different kinds of plasmon; volume plasmon, surface plasmon and localized plasmon, the last two are going to be discuss later. The volume plasmons are plasmons that are excited over a whole volume. These plasmons can be only excited in a longitudinal way and not in a transverse way like the surface and non localized plasmons. This means that the only way to couple a volume plasmon is by particle impact.

During the rest of the work we are going to talk about the other kinds of plasmon excitation; surface plasmon and localized plasmon. Despite volume plasmons, these excitations can be excited by a transverse wave, which can be for example light. This property makes them very useful and during this work we are going to show a variety of applications where this property is strongly employ.

ANALYSIS OF SURFACE PLASMON DEVICES (PLASMON WAVEGUIDE)

In this chapter we are going to analyze the Surface plasmons and their applications. During this chapter we are going to study their theory and also make simulations using MATLAB for its understanding. Afterwards we analyze the simplest surface plasmon system, which is the plasmon waveguide. We are going to calculate its losses and mode shapes using COMSOL with emphasis in their losses due to bending. This is done because as it is known, if plasmon waveguides become one day optical interconnections in an integrated circuit, possibly they would have to be bended, in order to interconnect different parts in a chip. Therefore a good understanding in how bending a waveguide will affect its losses is needed. We compare the bending losses of 4 different kinds of plasmon waveguides, which are well known in the literature [6-9]. At the end different graphs comparing them, showing which the best is, are presented.

ANALYSIS OF THE WAVE EQUATION FOR SURFACE PLASMON POLARITONS (SPP)

Surface plasmon polaritons (SPP) are electromagnetic excitations at the surface of a metal, generated by the interaction between an electromagnetic wave and the electron plasma in the metal. In order to fully understand their behavior, we have to start by solving the Maxwell equations in a dielectric-metal interface. Let us first start by writing the wave equation:

$$\nabla \times \nabla \times \vec{\boldsymbol{E}} = -\mu_0 \frac{\partial^2 \vec{\boldsymbol{D}}}{\partial t^2}$$

For simplifying the problem, we can suppose that we have an infinite surface in the direction of y and x. As said before, SPP are excited in a transverse way. Therefore we can suppose that the solution for the electric field is a transverse electromagnetic wave propagating in one direction parallel to the surface (For example the x direction). The solution of the electric field in this case is: $E = E(z)e^{i\beta x}$ taking into account that there would be only dependence in z because we are solving for an infinite plane. Applying this solution the wave equation becomes:

$$\frac{\partial^2 \overrightarrow{\boldsymbol{E}(\boldsymbol{z})}}{\partial z^2} + \left({k_0}^2 \varepsilon - \beta^2\right)\boldsymbol{E}(\boldsymbol{z}) = 0 \qquad (4)$$

This equation has two kinds of solutions: One which gives a TM-mode (transverse magnetic mode) and the other one which gives a TE-mode (transverse electric mode). The TE-mode is an electric field in a direction parallel to the surface and perpendicular to the propagation vector. This kind of field in fact will not exist in our case because if we apply the boundary condition at the surface to it, we will not have a confined mode. T Details of this can be found in [10]. Therefore in the following sections we are going to limit our analysis only to the TM-mode.

Dielectric-metal interface.

In this section we are going to solve (4) for the simply dielectric-metal interface. For simplicity we put the reference at $z = 0$ (z < 0 is dielectric and z > 0 is metal). Solving (4) for the TM-mode will lead to the next solutions for the electric and magnetic field: For $z \geq 0$

$$H_y(z) = A_2 \mathrm{e}^{i\beta x} \mathrm{e}^{-k_2 z}$$
$$E_x(z) = i A_2 \frac{1}{\omega \varepsilon_0 \varepsilon_2} k_2 e^{i\beta x} \mathrm{e}^{-k_2 z}$$
$$E_z(z) = -A_1 \frac{\beta}{\omega \varepsilon_0 \varepsilon_2} e^{i\beta x} \mathrm{e}^{-k_2 z}$$

And for $z < 0$:

$$H_y(z) = A_1 e^{i\beta x} e^{k_1 z}$$
$$E_x(z) = -iA_1 \frac{1}{\omega \varepsilon_0 \varepsilon_1} k_1 e^{i\beta x} e^{k_1 z}$$
$$E_z(z) = -A_1 \frac{\beta}{\omega \varepsilon_0 \varepsilon_1} e^{i\beta x} e^{k_1 z}$$

Here k_1 and k_2 defines the component of the wave vector perpendicular to the propagation. Their reciprocal value defines the decay length of the evanescent wave.

Application of the boundary conditions to the previous equations will demand that $A_1 = A_2$ and that:

$$\frac{k_2}{k_1} = -\frac{\varepsilon_2}{\varepsilon_1}.$$

Note that according to the signs of the previous equations, only if $Re(\varepsilon_1) < 0$ and $\varepsilon_2 > 0$, we would have a confine mode in the surface. Also in order to fulfill the wave equation we must have:

$$k_1^2 = \beta^2 - k_0^2 \varepsilon_1$$
$$k_2^2 = \beta^2 - k_0^2 \varepsilon_2. \quad (5)$$

If we solve the last three equations for β we get:

$$\beta = k_0 \sqrt{\frac{\varepsilon_1 \varepsilon_2}{\varepsilon_1 + \varepsilon_2}}.$$

During the whole work we are going to use gold as our metal material. In order to analyze in the best way our systems, and guarantee that our simulations give a real value, we take the real values of the gold permittivity. These values were found several years ago by Johnson and Christy [11]. Taking these values we plot using MATLAB the dispersion diagram for gold:

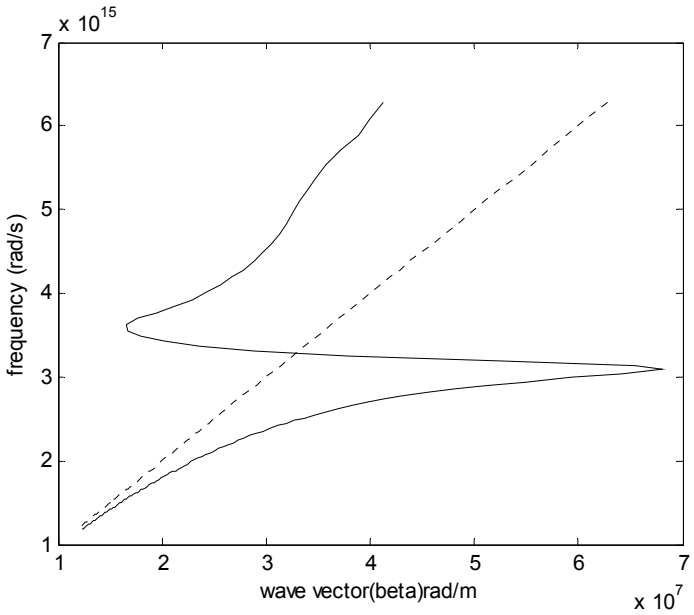

Figure 1.1. Dispersion diagram for gold. (dash curve) light propagating only in the dielectric. (dark curve) light propagating in a dielectric-gold interface. The dielectric constant is $\varepsilon_r = 9$.

In figure 1.1, we see clearly that there is a huge peak around $\omega = 3 \times 10^{15}$, this peak is the so-called surface plasmon frequency of the gold. In fact as the dielectric constant gets small, this peak becomes sharper and sharper, and the peak becomes less visible due to the small resolution of the values provided by Johnson and Christy. That's why for doing the dispersion diagram we choose to have a big value for the dielectric constant.

In the diagram we also see that there is a part of the black curve that goes before the dielectric line. This behavior is unphysical because it is impossible for a wave to propagate faster than the light propagating only in the dielectric. In order to understand this we also plot the propagation length, which is the length at which the electric field will decay 1/e of its amplitude or the reciprocal of the wave vector's imaginary part:

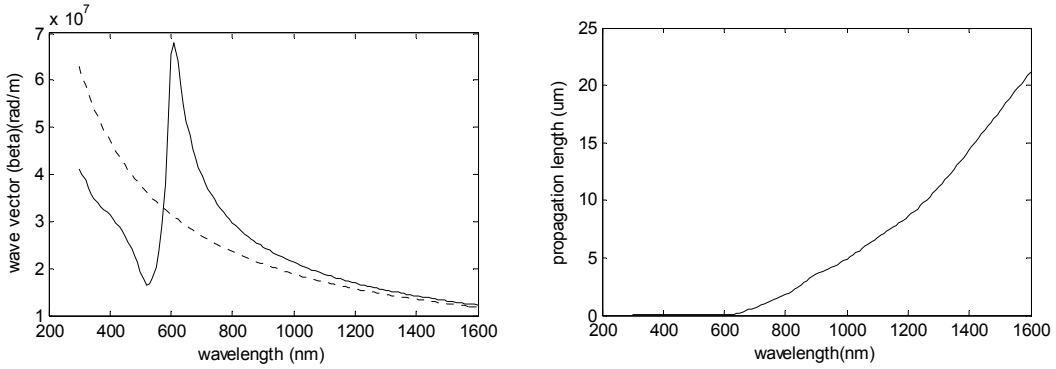

Figure1. 2. Left. Wave vector against wavelength. (dark line) Gold-dielectric interface. $\varepsilon_r = 9$. (dash line) light propagating only in the dielectric. Right. Propagation length against wavelength.

In figure 1.2, we can see that the propagation length (right figure) is almost zero before 600nm of wavelength. This means that in this region the losses are very high and almost there is no wave propagating. In figure 1.2 (left figure) we can see that this region coincides with the region where the wave vector goes before the dielectric line. So in fact this results corresponds to waves that are actually not propagating and don't exist.

From figure 1.2 (right figure), we can also see that around a wavelength 1400nm, we have a considerable propagation length. In fact, if we decrease the dielectric constant, we can increase also the propagation length to values around 500um. This value is in the order of the wire's length of actual electronic chips. That's why even if the losses of surface plasmon are very large compare to optical fiber losses; they still can be used in small systems as optical connections. In the next part, we are going to see how we can guide these surface plasmons.

For understand better the kind of modal shape that a plasmon mode will have as it propagates, we also compute the shape of the TM-mode from the solution of the wave equation(4) given previously. Figure 1.3 shows the results.

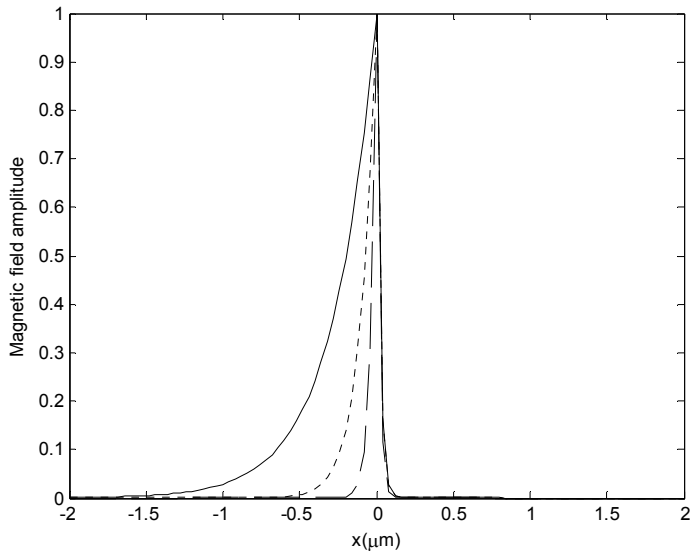

Figure1. 3. TM-mode profile for a plasmon mode in a dielectric-gold interface. $\varepsilon_r = 9$. (Straight line) $\lambda = 1550nm$. (Dotted line) $\lambda = 1000nm$. (Dashed line) $= 700nm$. $(x > 0)$ Metal.$(x < 0)$ Dielectric.

Dielectric-Metal-Dielectric (2 interfaces)

In order to guide SPP through a structure we need to have an enhancement of the SPP electric field in a certain area. According to figure 1.3, the TM-mode has an enhancement around the interface. So if we put a very thin film of metal instead, we are going to have the same enhancement in the interface, but this time around the area of the metallic thin film. How thin should be this metallic thin film? Later, in this chapter we are going to see the different consequences of decreasing and increasing this metallic thin film in film and that at

the end there is a certain trade-off in its thickness. For now let's focus on how actually SPPs behave in this metallic thin film. Checking the boundary conditions we see that actually there are two Dielectric-metal interfaces, and so two SPPs are going to be generated. These SPPs are going to interact between each other generating at the end a coupled surface plasmon. To find the wave vector and the modal shaped of this coupled SPP, we have to solve the wave equation and apply the boundary conditions in both interfaces. Details on the solution of this problem can be found at [10]. Here we are only interested in the fact that there are two different kinds of SPP modes that are going to propagate; odd modes and even modes. The equations describing the dispersion relation of the system are:

$$\tanh(k_1 a) = -\frac{k_2 \epsilon_1}{k_1 \varepsilon_2} \ (6.a)$$

$$\tanh(k_1 a) = -\frac{k_1 \epsilon_2}{k_2 \varepsilon_1} \ (6.b)$$

In the equations , a refers to the thickness of the metal layer. The sub index 1 and 2 are for the metal and dielectric respectively. And $k_{1,2}$ refers to the perpendicular evanescent component of the wave vector. Also, equation (6.a) describes the dispersion relation for odd modes and (6.b) for even modes. Using matlab and using the relations which relate the wave vector with k_1 and k_2 (5), we plot the dispersion relations for the odd and even modes:

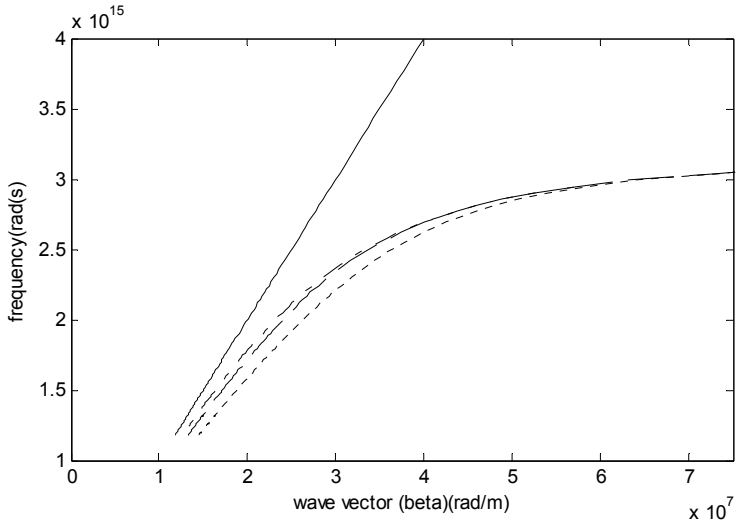

Figure 1.4. Dispersion diagram for the odd mode in a dielectric-gold-dielectric interface. . $\varepsilon_r = 9$. (dark curve) Light propagating only in dielectric. (dotted curve) thickness of 50nm. (dash curve) thickness of 100nm. (dotted-dash curve) thickness of 200nm.

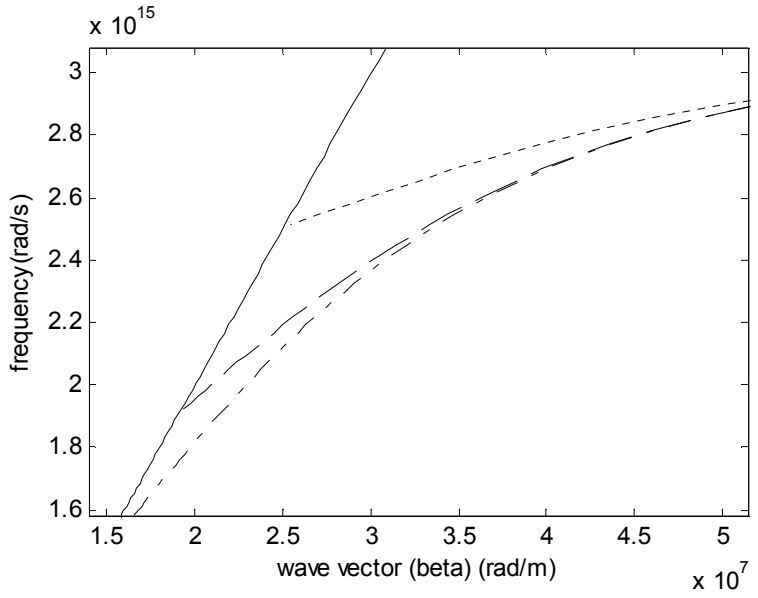

Figure 1.5. Dispersion diagram for the even mode in a dielectric-gold-dielectric interface. . $\varepsilon_r = 9$. (dark curve) Light propagating only in dielectric. (dotted curve) thickness of 50nm. (dash curve) thickness of 100nm. (dotted-dash curve) thickness of 200nm.

For understanding how the different modes behave against the thickness of the metal, we plot the dispersion diagram for different thickness. At frequencies around $\omega = 1.5 \times 10^{15}$, for odd modes, we find out that as the metal thickness decreases, It approaches more and more the light-line (dark curve in figure 1.4). This is reasonable because as the metal thickness decreases, more and more light will propagate in the dielectric. Nevertheless at a certain point there will be always the surface plasmon frequency region where losses become very large and propagation is limited. For the even modes we clearly see dependence in the thickness of the metal. In fact there is a cut-off frequency where these modes start to exist, and this cut-off frequency depends strongly on the thickness of the metal, so as the metal becomes thicker, this cut-off frequency will become closer to the plasmon frequency and these modes will have huge losses and will not propagate. Therefore, for thin metallic layers we will only have odd modes propagating on them.

Using MATLAB we also plot the TM even and odd mode of our system:

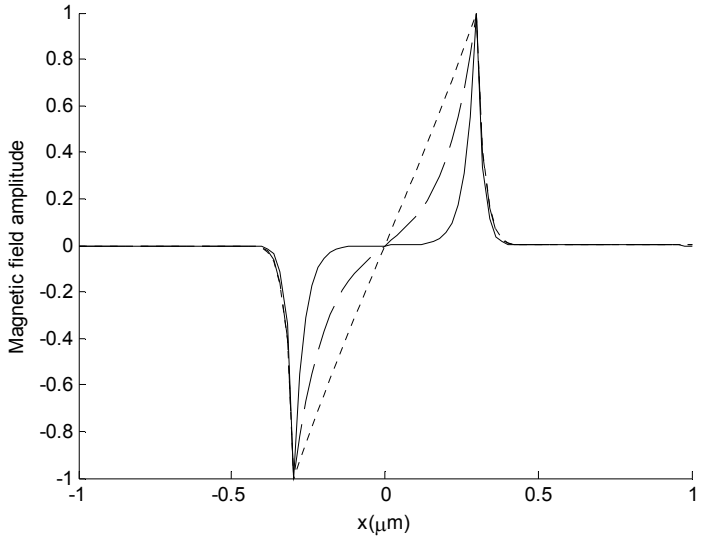

Figure 1.6. Even Mode profile for a dielectric-gold-dielectric interface. $\varepsilon_r = 9$. (dotted curve) $\lambda = 1500nm$ (dash curve) $\lambda = 1000nm$. (dark curve) $\lambda = 700nm$.

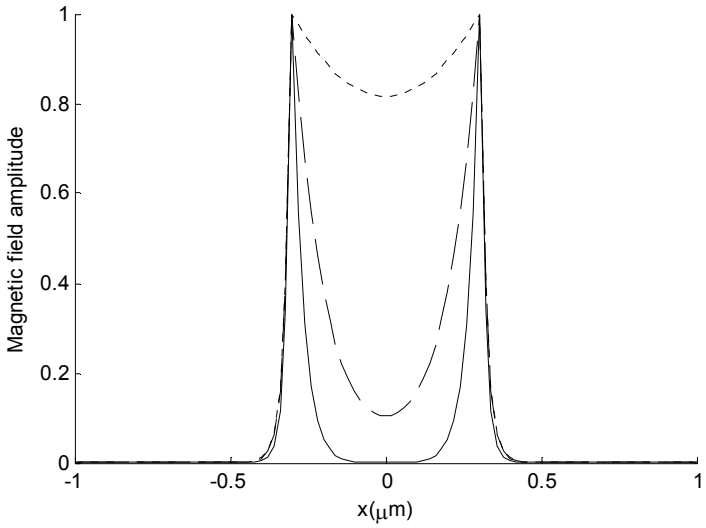

Figure 1.7. odd Mode profile for a dielectric-gold-dielectric interface. $\varepsilon_r = 9$. (dotted curve) $\lambda = 1500nm$ (dash curve) $\lambda = 1000nm$. (dark curve) $\lambda = 700nm$.

For the odd mode, we can see that as the wavelength increases, also the mode amplitude inside the metal increases. In fact, if we reduce the thickness of our metal layer to a thickness around 100nm, we are going to see that the mode profile will become almost flat at the value of one for the wavelengths of 1500 and 800nm. In practice, the thickness of the metal layer is usually quite small, in order to have not only a high field amplitude in the metal layer, but also to avoid the generation of even modes, which will lead to multimode behavior and the increase of our system losses.

The last thing that we have to calculate for the total understanding of our system is its propagation losses. Unfortunately, finding the losses of even a simple system as a dielectric-gold-dielectric is very difficult. It requires solving complex equations with not so obvious solutions as in the case of the dielectric-gold interface. So in this case we are going to use a FEM (finite element method) for this purpose, and we are going to compute the losses of different kind of plasmon waveguides. Furthermore, we are going to compute the losses also coming from the bending of a waveguide. These losses are very important as said before, if these waveguides will one day become part of an integrated chip.

ANALYSIS OF LOSSES IN DIFFERENT KINDS OF PLASMON WAVEGUIDES.

An important figure of merit for characterizing a waveguide is the losses. The losses determine the waveguide reliability and give a value for its maximum propagation in certain media. As seen before, plasmon waveguides have huge losses due to the metal. Nevertheless in the case of a dielectric-gold interface, there is still a quite considerable propagation length despite the gold losses. We will see that this propagation length can be later improved by changing the geometry of our system to a dielectric-gold-dielectric interface. In fact having a very thin gold film in our waveguide will reduce the amount of losses because actually we are reducing the amount of gold in our waveguide. Nevertheless, care must be taken because if we reduce greatly the thickness of the gold film we will lose the mode confinement and as we will see later; this behavior is not desirable, overall when we are dealing with bending losses. During this part the analysis of the modes and the losses will be computed for $\lambda = 1550nm$, because we are going to focus our analysis for telecom applications and this is the working wavelength.

Losses simulation using COMSOL Multyphysics.

As said before, for calculating the losses we are going to use a program which implements the finite element analysis. This program is called Comsol multiphysics [12]. By using this program we can obtain the imaginary part of the wave vector and then compute its reciprocal to get the propagation length. This can be easily done if we compute the wave vector for a straight waveguide. Unfortunately, computing the wave vector for a bended waveguide is not so easy. COMSOL uses rectangular coordinates for computing the mode. The propagation direction is defined in the z axis, and the mode is calculated in the xy plane. In the bended waveguide case, we have a cylindrical coordinate's problem. Our mode is going to propagate in the θ direction and the solution of our mode will be in the rz plane. Therefore we have to change the coordinates of our problem in order to allow COMSOL to solve it.

COMSOL relate the magnetic and electric fields via the curl of the electric field define as:

$$\nabla \times \begin{pmatrix} E_x \\ E_y \\ -\alpha e_z \end{pmatrix} e^{\alpha z} = \begin{pmatrix} -\alpha(E_y + \frac{\partial e_z}{\partial y}) \\ \alpha(\frac{\partial e_z}{\partial x} + E_x) \\ \frac{\partial E_y}{\partial x} - \frac{\partial E_x}{\partial y} \end{pmatrix} e^{\alpha z} \quad (7)$$

Details in why COMSOL put the electric field in this way can be found in help of COMSOL. Here α is the eigenvalue for which COMSOL solves the problem. Also α is defined as $\alpha = i\beta$

where β is the magnitude of the wave vector. This eigenvalue is a complex number and its real part will give us the imaginary part of the wave vector which is what interests us. The curl in cylindrical coordinates is given by:

$$\nabla \times \begin{pmatrix} A_r \\ A_y \\ A_\theta \end{pmatrix} = \begin{pmatrix} \frac{\partial A_\theta}{\partial y} - \frac{1}{r}\frac{\partial A_y}{\partial \theta} \\ \frac{1}{r}\frac{\partial A_r}{\partial \theta} - \frac{\partial (r A_\theta)}{\partial r} \\ \frac{\partial A_y}{\partial r} - \frac{\partial A_r}{\partial y} \end{pmatrix}$$

For applying this new curl to the electric field defined by COMSOL, we also need to define a new eigenvalue. This new eigenvalue is $\alpha_r = \alpha r_0$ where r_0 is the bending radius of our waveguide. So in this case $e^{\alpha z}$ becomes $e^{\alpha_r \theta}$, and the curl of the electric field becomes

$$\nabla \times \begin{pmatrix} E_x \\ E_y \\ -\alpha_r e_z \end{pmatrix} e^{\alpha_r \theta} = \begin{pmatrix} -\alpha_r \left(\frac{\partial e_z}{\partial y} + \frac{1}{r} E_y \right) \\ \frac{\alpha_r}{r} \left(E_x + e_z + r \frac{\partial e_z}{\partial x} \right) \\ \frac{\partial E_y}{\partial x} - \frac{\partial E_x}{\partial y} \end{pmatrix} e^{\alpha_r \theta} \quad (8)$$

By changing this result for the pre-defined curl in COMSOL (7), multiplying the volume differentials by r, and changing r by $x + r_0$, we can allow COMSOL to solve problems using cylindrical coordinates. Nevertheless, in order to have the good value for the wave vector still there is one other thing to do. When we simulate our structure, usually when approaching very small curvature radius, we find out that part of the wave will radiate in the r direction. Unfortunately our geometry in the simulation is finite in both r and y directions. So when the wave start to radiate towards the r direction, the boundary conditions in the geometry borders will make the wave to reflect and interfere with the actual mode giving us a wrong wave vector number. In order to solve this kind of problem, we use a PML (perfectly matched layer). A PML is a layer that will match our media in order to avoid reflections. This kind of layer will allow us to simulate an infinite space even if our domain is finite, and to compute the good wave vector for our waveguide. There are different ways to implement a PML. In this work we are going to use an anisotropic PML, which is the same kind of PML used in [ref-13]. The details in the selection of this kind of PML can be found in [ref]. For the construction of the PML we consider a layer having a permittivity and permeability tensor defined as:

$$[\epsilon]_{PML} = \varepsilon[\Lambda] \text{ and } [\mu]_{PML} = \mu[\Lambda]$$

Where

$$[\Lambda] = \begin{bmatrix} \frac{s_y s_z}{s_x} & 0 & 0 \\ 0 & \frac{s_z s_x}{s_y} & 0 \\ 0 & 0 & \frac{s_x s_y}{s_z} \end{bmatrix}$$

In our case, it has been shown [14] that the values for $s_{x,y,z}$ are:

$$\begin{cases} s_x = c_r \\ s_z = \frac{\tilde{r}}{r} \\ s_y = 1 \end{cases} \quad \text{with} \quad \tilde{r} = r_0 + \int_{r_0}^{r} s_x(r')dr'$$

Here c_r is a complex number which defines the absorption profile that our PML will have. A highly used profile [13,15-16]:

$$s_x = 1 + i\left(\frac{x - x_0}{L}\right)^2 \delta_{max}$$

Here L is around 1 or 2 wavelengths and x_0 is the starting point of the PML. Also δ_{max} is defined as the maximal absorption achieved by the PML. Here we choose a value of 2 for it, in agreement with many other publications.

Simulation of the four kinds of plasmon waveguide.

At this point we have already the tools to compute the losses in a waveguide (for both straight and bended case). So we decide in order to use them, to analyze different kinds of surface plasmon waveguides, in order to find out the different advantages and disadvantages of each of them when used as optical interconnections in a chip. This study will help us to understand the different considerations in the design of these optical interconnections according to its final application. For the realization of this study we decide to analyze the losses at different curvatures radius where the analysis for big curvature radius will give us also the analysis for the straight case. We choose 4 different kinds of waveguides. These waveguides are widely documented in the literature, and have been analyzed for its losses giving a good performance [6-9].

The different kinds of waveguides chosen for the analysis are described in figure [8]. As said before all test were made at $\lambda = 1550nm$ where the complex permeability of gold is $\varepsilon = -114 + 11i$. The dielectric employed this time for the analysis is BCB which refractive index is 1.535. We use this dielectric because it was also used for the characterization of the rectangular waveguide [6] and we decide to also characterize the other different kind of waveguides with this dielectric in order to have the same conditions for each one. The rectangular waveguides (Fig 1.8. Right and left top) have a SPP mode that is going to propagate in the gold strip as it is supposed from the previous calculations. The difference between the two types is that the waveguide with a BCB layer surrounding the gold strip (Fig 1.8. Left top) will have a very good confinement due to the wave guidance realized by the two air-dielectric interface. Therefore this kind of structure will lead to a larger propagation length with respect to the other kind of rectangular waveguide (Fig 1.8. Right Top) The groove waveguide has two kinds of SPP modes, channel mode and wedge mode. The first one will propagate between the two metal interfaces of the groove, which will confine the mode and give it a large

propagation length. Meanwhile the wedge mode will propagate in the top corners of the groove, and will be weakly confined. The last waveguide is called a dielectric loaded surface plasmon polariton waveguide (DLSPPW). This waveguide will guide its SPP mode through squared dielectric waveguide in its top. This waveguide has a disadvantage. The thickness of the gold film in the bottom of the dielectric waveguide should be very large in order to confine the SPP mode in the dielectric; this will lead to large losses and very small propagation length

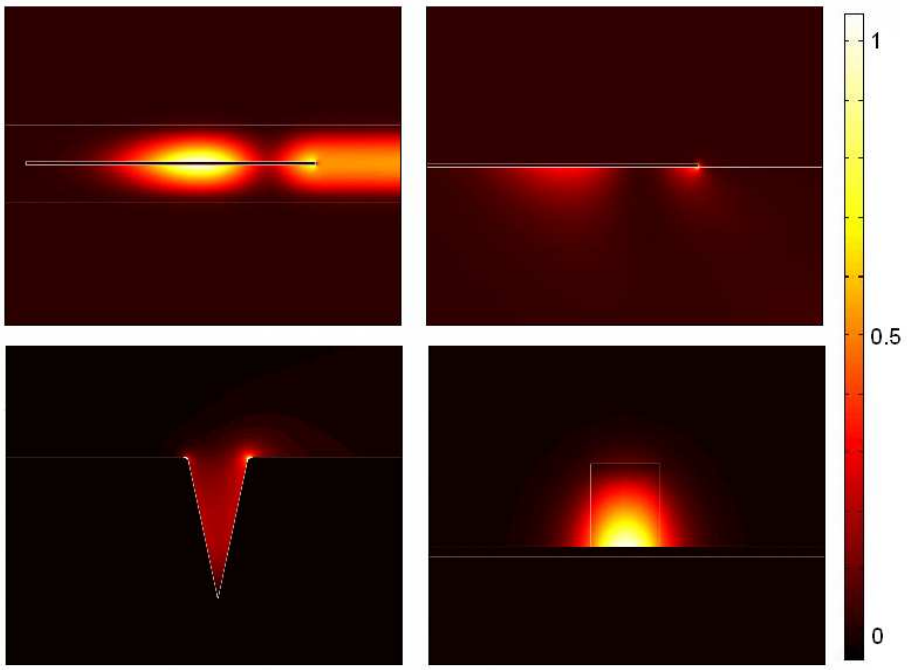

Figure1. 8. Modal shapes of the different types of waveguides at a bending radius of 100μm (Left top)Au strip of 70 nm and 6μm of width, inside of a BCB layer of 1.6μm of thickness; (Left bottom) Groove waveguide in Au substrate with height of 3μm and 25 degrees of aperture; (Right top) Au strip of 70 nm and 6μm of width, on a BCB substrate; (Right bottom) DLSPPW made of BCB with height of 600nm and width of 500nm on a layer of 100nm of Au.

All the waveguides were designed according to the previous studies [6-9]. For the case of the groove waveguide, it was shown in [7] that it is needed to have the groove covered either by a whole substrate of gold or an thick enough layer which simulates the same condition. In this case the wave will be strongly confined in the groove and will lead to the highest propagation length. The thickness of this layer was found to be 70nm or bigger. Also we decide to choose the same angle employed in [7,9], meanwhile for the height of the groove, we choose to have a height enough to confine and guide the channel SPP mode around λ=1.55μm, therefore we choose 3μm in agreement with previous publications[7,9].

Exactly the same case occurs in the DLSPPW waveguide [8], the gold layer under the dielectric waveguide has to be thick enough in order to strongly confine the mode in the dielectric. This thickness is around 100nm and will simulate the same effect as if we have a whole substrate made of gold. For the dimensions of the dielectric waveguide it was already

said in [8,17] that for a refractive index of around 1.5 in telecom applications (λ=1.55μm), the optimum dimensions for the dielectric waveguide were 600nm height and 500nm width according to previous simulations.

During the simulations for the design of the rectangular waveguides we find out that if we decrease the thickness the mode will become less confined, and will lead to larger losses. In the contrary if we increase too much the thickness we are going also to have more losses due to the absorption of gold. In order to show this we made some simulations for different layer thickness given a certain curvature radius [figure 1.9]. We see that there is an optimal thickness at which we get the maximum propagation length. Nevertheless in order to compare the behavior of these kinds of waveguides with the other waveguides. We decide to have a thickness which more or less generates the same losses as in the case of the groove waveguide. Therefore according to the simulations we decide to have 70nm as the thickness for both rectangular waveguides.

In figure 1.8 for the case of the groove waveguide we only plot the channel mode because despite the fact that its losses without bending are comparable with the other kind of waveguides, as we start our analysis for the bending losses we find out that its losses were too high and that its analysis was useless.

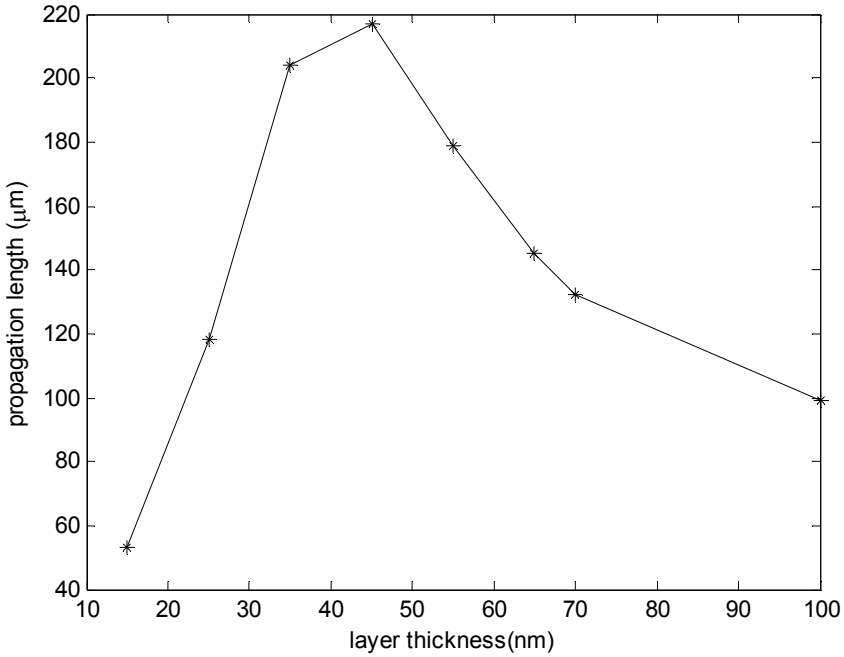

Figure1. 9. Propagation length against layer thickness for a rectangular plasmon waveguide with dielectric layer. The curvature radius is 200μm.

Figure 10 shows the waveguides losses for different curvature radius. During our simulations we find out a strange behavior for the case of the rectangular waveguide with dielectric layer. In fact we see that as bending radius start to decrease the propagation length increase a little bit until at a certain point in decays strongly. Mode profile of the modes at radii of 100μm and 200μm are shown. We see that as the bending radius becomes lower the mode is going to move towards the right (r direction) but at a certain radius the mode losses its confinement

from the strip and radiates to the outside. This mode radiation will be immediately guided by the air-dielectric-air interface to the outside making it easy for the SPP mode to leave the waveguide. This is not the case for the other kind of rectangular waveguide, where there is a dielectric-metal layer towards the outside which can't easily guide light. That's why this kind of waveguide has better behavior in small radii than the rectangular waveguide with a dielectric layer.

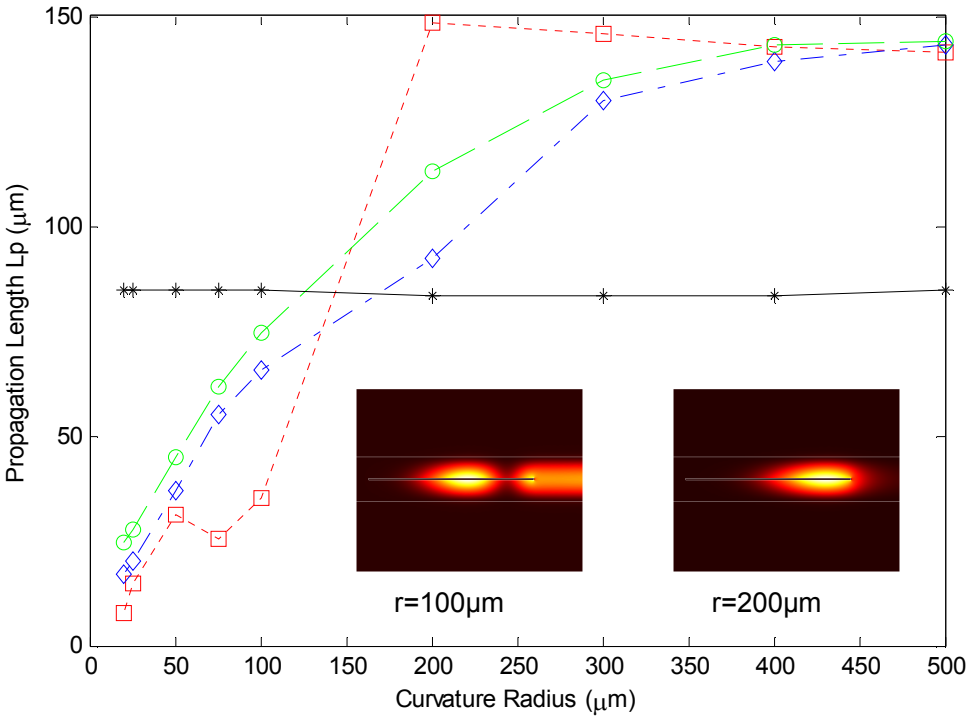

Figure 1.10. Propagation length for various curvature radiuses. (Red dotted curve) Rectangular strip in a Dielectric layer; (Green dash curve) CPP mode of a Groove Waveguide; (Blue dash-point curve) Rectangular strip on a Dielectric surface; (Straight curve) Dielectric Loaded Surface Plasmon Polariton Waveguide; Insets, Modal shape of the fundamental Plasmon mode for a rectangular strip in a dielectric layer for curvature radius of 100μm and 200μm. The lateral size of the insets is 8μm.

However the groove waveguide has better behavior due to the confinement in the metal-dielectric-metal interface but still the difference is not very high. . In the case of the DLSPPW the behavior is totally different. As we say before at larger radius we see that only the DLSPPW has larger losses due the higher thickness of the thin film. However as we see from Figure 1.10. It has a very nice behavior against bending losses. It has almost the same losses for every bending radius, even for the smallest ones. The principal characteristic of the DLSPPW which explain this behavior is the dielectric waveguide which is on top of the gold layer. In fact is in this waveguide where the SPP mode is going to be guided and strongly confined to the region in the waveguide. The dielectric-air interface will not allow the mode to radiate and go outside. This behavior has already been documented for splitters and interferometers at a very low scale [17]. Also a DLSPPW is very easy to fabricate as we can see from its shape (Figure 1.8 (bottom right)), which is a strong advantage against other type of waveguides like the groove waveguide. Figure 1.11 shows the propagation angle, which

is defined as the maximum angle reachable during a propagation length or the ratio between the propagation length and the curvature radius.

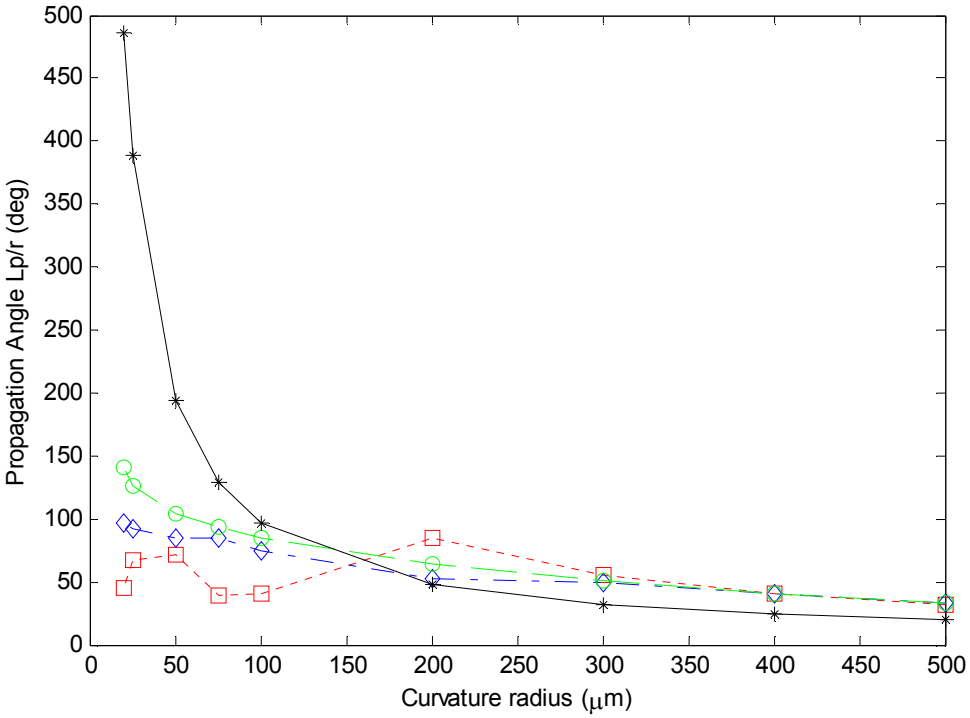

Figure 1.11. Propagation Angle (Propagation length over curvature radius) for various curvature radiuses. (Red dotted curve) Rectangular strip in a Dielectric layer; (Green dash curve) CPP mode of a Groove Waveguide; (Blue dash-point curve) Rectangular strip on a Dielectric surface; (Straight curve) Dielectric Loaded Surface Plasmon Polariton Waveguide.

As we said before the reachable angle for a DLSPPW is very high meanwhile for the others the highest angle is obtained by the groove waveguide. In conclusion, we have shown that there is a trade-off between the losses with and without bending. Regarding the losses without bending we saw that the rectangular waveguides and the groove waveguide show a good behavior at lower curvature radius, which is exactly the same case, nevertheless we also shown that the rectangular waveguides can be even improved and its losses can be reduced furthermore. In the case of the losses with bending we saw that in order to enhance the confinement of the SPP mode we must increase the thickness of the metallic layer which confines the generated plasmon, but care must be taken in order to not the losses of the system. This means that there is an optimal thickness for ensuring a good performance according to the use and application. However in order to reach very small curvature radius, we see that there is also needed a “barrier” for prevent the radiation of the mode to the outside, as it is the case of the DLSPPW. Indeed the DLSPPW seems to be a very promising SPP waveguide for bending applications (like integrated on chip optical interconnections) at very small scale.

ANALYSIS OF LOCALIZED PLASMON DEVICES (PLASMON NANOANTENNA)

In this chapter we are going to study the theory and the main applications of localized plasmon. We will realize different simulations for understanding their behavior, using the green's tensor method. We will design a dipolar nanoantenna using localized plasmon and we will give an explanation of the main parameters in order to achieve the best design. The dipolar nanoantenna will be excited by the evanescent field of a waveguide under the nanoantenna. Therefore the design of this waveguide and how its dimensions can affect the response of our nanoantenna will also be treated. Then a fabrication process for the elaboration of the nanoantenna will be shown and we will analyze some particular remarks for each step of the process. Later, for the testing of our nanoantennae we will design an experimental setup.

ABSORPTION AND SCATTERING OF SUBWAVELENGTH METALLIC PARTICLES

Localized plasmons are plasmons which are confined in very small regions and don't propagate as in the case of the surface plasmons. Nevertheless due to the very confined plasmons, the oscillation generated by the electron-sea will create electromagnetic waves which then can propagate making visible the plasmon. Due to this "antenna" behavior in the optical regime and to the large enhancement of the field in small regions, these plasmons have become a very good candidate for extremely sensitive detection, like single-molecule detection or surface enhanced Raman spectroscopy.

Nevertheless we still have to generate these Localized plasmons in order to take advantage of these effects. We can obtain localized plasmon by exciting with an electromagnetic wave, sub wavelength metallic particles. The reason why these particles must have a size smaller than the wavelength of excitation is to have a constant phase of the field over the whole volume of the antenna. This will polarize all the electrons in the volume in the same and with the same amplitude.

Analysis of Individual plasmon systems.

To start our analysis let us first consider a spherical particle with a size smaller than the wavelength of excitation. Due to the size of the particle, we can say that the field in the whole particle is constant as we say before. In this case we just have to solve the electrostatic problem for the particle in a constant electric field. Figure 2.1 shows this case.

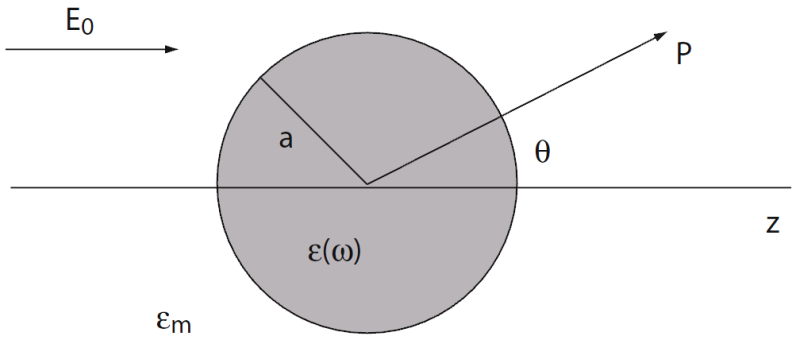

Figure 2.1.Spherical particle in a constant electric field.

It can be shown [10] that the potential outside of this particle is:

$$\Phi_{\text{out}} = -E_0 r\cos\theta + \frac{\mathbf{p}\cdot\mathbf{r}}{4\pi\varepsilon_0\varepsilon_m r^3}$$

With:

$$\mathbf{p} = 4\pi\varepsilon_0\varepsilon_m a^3 \frac{\varepsilon-\varepsilon_m}{\varepsilon+2\varepsilon_m}\mathbf{E}_0.$$

Here we see that there is a dipole moment in the field of the small particle which can be greatly enhanced if the denominator vanishes, this condition is:

$$\mathrm{Re}\left[\varepsilon\left(\omega\right)\right] = -2\varepsilon_m .$$

This condition is called the Fröhlich condition and it is at this condition where not only the dipole moment is enhanced but also the electric field around the particle. From Fröhlich condition we can see that the resonance of the particle depends strongly of the surrounding media. This means that this kind of system has a very high sensibility against the change of media and it is here where the localized plasmon has their application in biology sensing.

Analysis of coupled plasmon systems.

Coupled systems are systems of two or more metallic particles which are closer enough to have their near fields interacting. As we saw previously, in the simple case of a spherical particle, we are going to have a dipole behavior with a depolarizing electric field in the outside. If we add more of these particles and we put them together to interact, the field generated by the charges of the neighbor is going to attract or repel the electrons of the metallic particle increasing or decreasing the electron's effective mass. This change in the effective mass will originate a shift in the resonance frequency. For example if we have a line of spherical particles and we excited them with different polarization (Figure 2.2), we will obtained that in the case of the transverse polarization we are going to have a repelling field between the charges in the neighbors generating a blue shift for the plasmon resonance meanwhile in the other case we are going to have a red shift.

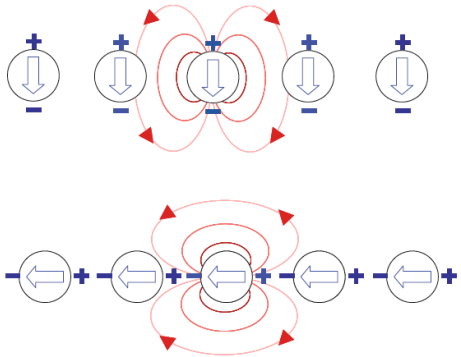

Figure 2.2. Line of spherical particles excited with different electric field polarization. (up) Transverse polarization. (down) longitudinal polarization.

The electric field between two neighboring particles is greatly enhanced due to the superposition of the fields coming from both particles. In fact this effect is even bigger than the normal effect in a single particle and can lead to applications like optical trapping.

DESIGN OF THE DIPOLAR NANOANTENNA

In this part we are going to design a Dipolar Gold Nanoantenna with the purpose of generate localized plasmons at a wavelength of the 1.550μm in order to fabricate Gold nanoantennae for telecom applications. These nanoantennae are going to be excited by the evanescent

field of a TM-mode in a planar waveguide. This planar waveguide is going to be realized using silicon and silicon oxide which are widely used materials in clean room

Analysis.

. A schematic showing the configuration of our planar waveguide is shown in figure 2.3.

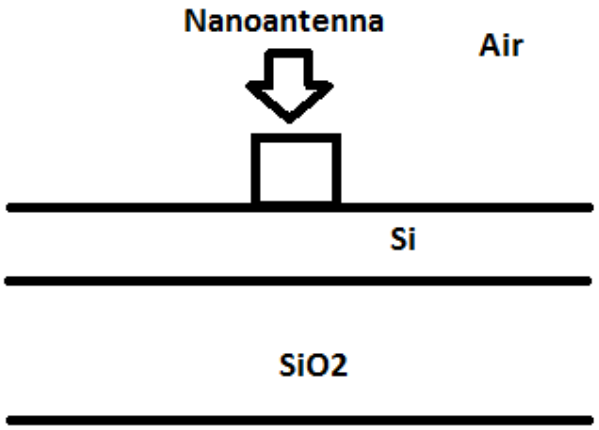

Figure 2.3. Configuration of our planar waveguide, the light will propagate as a guided mode in the Si layer and its evanescent field at the air interface will excite our nanoantenna.

In order to have a single mode condition for both TE and TM modes, we decide the thickness of our waveguide according to the equation for the number of modes:

$$M = 2\frac{d}{\lambda_0}NA \quad with \quad NA = ({n_1}^2 - {n_2}^2)^{1/2}$$

These equations are meant for the symmetric planar waveguide. Here 1 and 2 are the sub index for the guiding layer and the outside layer λ_0 is the wavelength and d is the thickness of the guiding layer. As we can check from figure 2.3, our waveguide is not symmetric but it is an anti-symmetric planar waveguide. So in order to apply these equations we choose a certain value of thickness and then we calculate the number of modes for silicon oxide and air according to the thickness chosen. Then given the value of M for each case we can check if our thickness allows or not only one mode. The value chosen for the thickness was 400nm because it is close to the ratio between the wavelength and the refractive index. We compute the modes for this thickness and we find out 1.72 for the case of air and 1.63 for the case of the silicon oxide. In effect, for a symmetric waveguide these numbers will mean that there is at least two modes because the M=0 mode is allow. In the case of an anti-symmetric waveguide, this mode is not allowed and according to these numbers there would be only one mode allowed. One important thing is that this equation is valid for both polarizations; TE and TM. Therefore at the end we will have two modes; one TE and one TM.

Having the thickness of our waveguide, we proceed to design of the gold nanoantenna. The shape of the nanoantenna is shown in figure 2.4. This shape has already been analyzed in [18,19]. The two rectangles are going to behave as a couple system where at the plasmon resonance of each of the arms the electric field in the gap is going to be greatly enhanced.

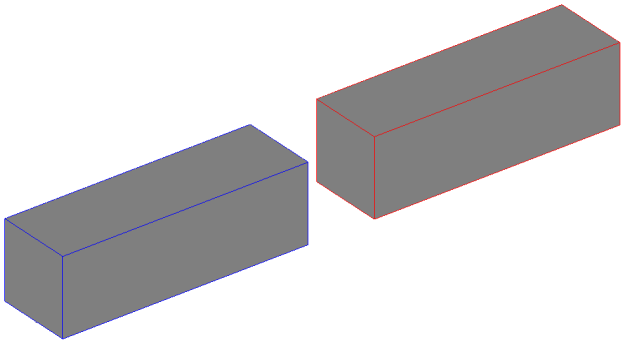

Figure 2.4. Shape of the gold nanoantenna

In order to design the dimensions of the nanoantenna, we use a simulation program call scatly3d which uses the green tensor method [20]. Using this program we compute the absorption of the nanoantenna for different wavelengths in order to check where was the absorption peak corresponding to the plasmon resonance. Then we start to change the dimensions in order to tune this peak to our testing wavelength; 1.55μm. We start with a similar design as the one used in [19]; we design our nanoantennae to have a width and thickness of 40nm and then we vary the length for tuning the plasmon resonance. During the simulations we find out that scatly3d makes the computation very slowly for a waveguide mode and it would take a long time for compute the response of the nanoantennae at each wavelength. Instead we use scat3d which uses the same method as scatly3d but with exception that it can only compute the field for an infinite substrate instead of a layer like our case. Therefore in order to simulate the same case we add a certain incidence angle to our electric field. Figure 2.5 shows this case.

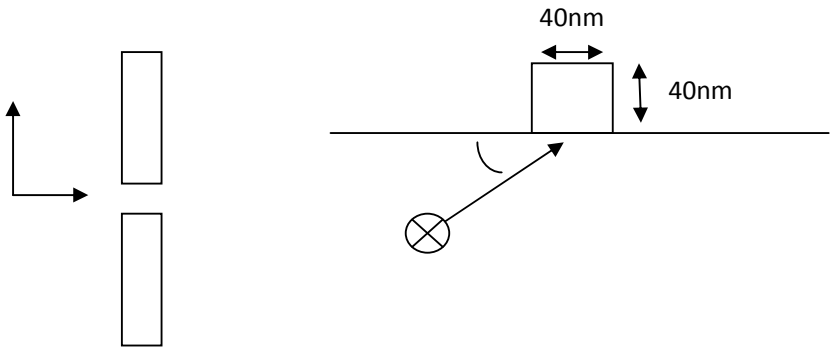

Figure 2.5. Change of the simulation for the use of scat3d. (is the angle of incidence)

As we know, light is going to be guided in the thin layer. This behavior can be understood in two ways. One is to think that light is a plane wave bouncing between the boundaries with a wave vector depending only in the refractive index where it propagates. Or two is to think that light is a wave guided mode with a wave vector depending on the effective refractive index. The two ways are acceptable and in fact the angle of incidence that we are looking for is the same angle at which the planar wave arrives in the first case, because this angle will simulate the same condition as if it were a waveguide. One remark is that the wave for both

models will propagate the same distance. This means that there is a relation between the two models for their wave vectors:

$$k_2 = k_1 \cos(\theta_i) \quad or \ \cos(\theta_i) = \frac{k_2}{k_1}$$

Where 1 and 2 corresponds to the corresponding models defined before. Here we can express the relation between the two wave vectors in function of the refractive index and the effective refractive index. The result is:

$$\cos(\theta_i) = \frac{n_{eff}}{n}$$

Where in our case n is the refractive index of silicon which is 3.48 and the effective refractive index is going to be 3.27 according to a simulation of the waveguide using COMSOL.
Thereby using the previous equation we find out an incidence angle of 20 degrees.

Simulation

Given this angle we start our simulation. The codes used in scat3d and scatly3d are shown in annex 1. We start by varying the length of the nanoantennae for placing the absorption peak in the wavelength that we want to. We discovered that a length of 130nm will have a resonance peak around 1500nm and a change of 10 nm of this length will become a change of 150nm in the resonance peak wavelength. This means that having our nanoantenna exactly focus around 1550nm is very difficult because it will require a precision of 1nm in the design and that in terms of fabrication will be very difficult. At the end we decide to leave the 130nm length for our nanoantenna and then after in the fabrication we are going to produce different nanoantenna with lengths varying 5 nm from 130nm in order to check which could be the one with the best response at 1550 nm.

First of all we simulate the behavior of our nanoantenna according to the gap. The results are shown in figure 2.6. As was predicted before, as the nanoantenna's gap decrease, the amplitude of the electric field in the gap increase and there is an enhancement in the peak of absorption. Also we see that at a value of 20nm of gap we have also a little red shift of the peak which can be understood in the same way as for the couple spherical particles. According to the figure having a 20nm gap will be the best gap for our nanoantenna because it has the highest response at 1.55μm. However reaching such small gap is usually very difficult for the equipment used for the fabrication (electron beam). So instead we decide to choose a 30nm gap nanoantenna. Nevertheless during the fabrication we also try to realize a 20nm gap nanoantenna.

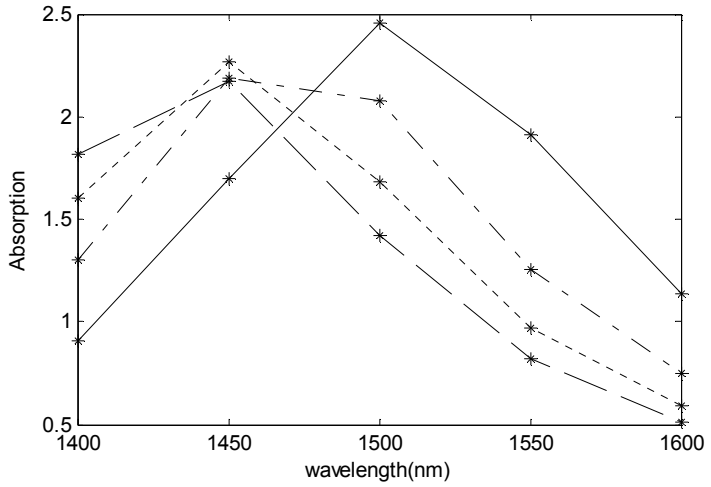

Figure 2.6. Nanoantenna absorption at different gap size (width and thickness are 40nm and the length is 130nm)(straight line) 20nm (dash dotted line) 30nm (Dotted line) 40nm (dash line) 50nm

Finally we also study the effects of varying the width, the thickness. For the width and the thickness when varied alone we obtain just a shift in the resonance frequency. But when vary together we start to obtain a very strange behavior. Instead of having one peak we obtained two peaks (Figure 2.7). This behavior can be understood if we suppose that there is a transverse excitation for the free electron gas in the nanoantennae. This transverse excitation, which is perpendicular to the TM polarized electric field exciting the nanoantennae, will make the electron gas to bounce between the faces of the nanoantenna larger rectangle generating different kinds of modes according to the width and thickness of the nanoantenna (like for example in a waveguide where it is light that bounce between the interfaces).

There are two possible causes for this transverse excitation. The first one is a consequence of the fuchs theory [21]. Fuchs years ago calculated the absorption spectrum of cube particles of ionic crystals, e.g. NaCl. In his work he calculates the absorption spectrum from the electrostatic solution of the system (like we show before for the case of the spherical particles) and he discovered that a cube structure will have at least 6 important resonances in its absorption spectrum. Indeed, when we solve the electrostatic problem for a cube, we will find that there is a strong enhance of the electric field around the corners of the cube. Due to this enhancement in the corner, this electric field will have a radial component. Therefore this radial component will have a transverse component, generating a transverse excitation. The second one is just simply a consequence of the transverse component of the electric field due to the losses of the gold. In this case we think that this component is less important due to the dimensions of the nanoantenna.

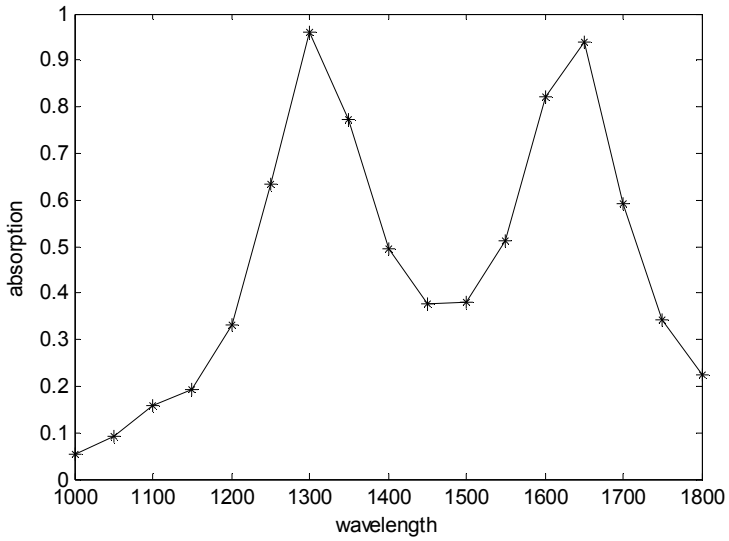

Figure 2.7 Absorption spectrum for the nanoantenna with a width and thickness of 50nm. (length is 130nm and gap is 30nm)

Results

Figure 2.8 shows the response of our nanoantenna with the designed thickness (40nm width, 40nm thickness, 130nm length and 30nm gap) using this time scatly3d and computing it with a waveguide mode. As can be seen from the figure, we only compute just few points due to the large computation time that the program takes. Nevertheless we can see that our design generates a great enhancement of the absorption around 1500nm as expected and there is still a very good absorption at 1550nm despite the fact that the dimensions are not designed for make the nanoantenna resonate exactly at 1550nm.

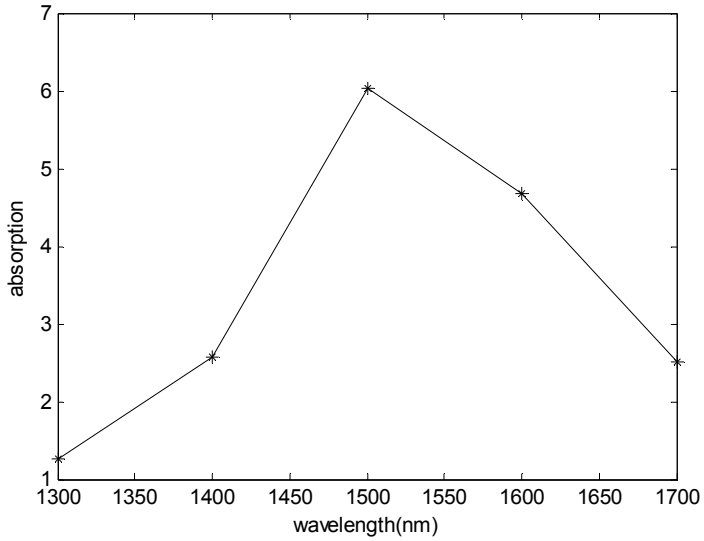

Figure 2.8. Absorption of the designed nanoantenna computed with scatly3d for the waveguide mode (40nm width, 40nm thickness, 130nm length and 30nm gap)

FABRICATION OF THE NANOANTENNA

The fabrication of the nanoantenna was done in the center of micro-nanotechnology (CMI) at the EPFL using the clean-room facilities. The substrate chosen for the deposition of the silicon and the posterior deposition of the nanoantenna was a silicon substrate with 500nm of silicon oxide on top. After the measurements we change to a whole silicon oxide substrate, we will explain after the reason.

We decide in order to see the radiation of the nanoantenna to write a word with them. So we also built a mask using a program called L-EDIT, which is specialized in layout design. The design of the mask is schematically represented in figure 2.9 where for each table cell, we add the words “LIGHT” and “LUZ” written with nanoantennae.

100nm gap 30nm	110nm gap 30nm	120nm gap 30nm
140nm gap 30nm	130nm gap 30nm	150nm gap 30nm
130nm gap 25nm	130nm gap 20nm	130nm gap 35nm
130nm gap 40nm	130nm width 50nm	130nm width 30nm

Figure 2.9. Schematic representation for the mask realized in L-EDIT. The first dimension in each cell is the length of both nanoantenna rectangles. Then when only “gap” is indicated, it means that the width is hold to 40nm and in the case when “width” is indicated it means that the gap is hold to 30nm. In all cases the thickness is 40nm.

In the schematic, we choose to vary the length in steps of 10nm for the nanoantenna and vary the gap in steps of 5nm. In this way we characterize the different response of the nanoantenna according to the variation in the dimensions. We also add a variation in the width in order to check also for the frequency shift predict by the simulations.

Here is the process flow for the fabrication of the nanoantenna (Figure 2.10)

1. The deposition of the 400nm thin film of silicon was made by LPCVD (low pressure chemical vapor deposition).
2. The obtained substrate is spin coated with a special resist used for the E-beam exposition (PMMA).
3. Exposition with the E-beam at a dose going from 650 $\mu C\ cm^{-2}$ to 810 $\mu C\ cm^{-2}$ in steps of 10 which means that we print 16 times the schematic represented in figure 2.9 and posterior developing of the resist
4. 8 seconds Oxigen plasma etching in order to remove the remaining resist.
5. Evaporation of 40nm of gold
6. 24 hours bath on acetone which will remove the resist removing also the gold on top. (Lift-off)

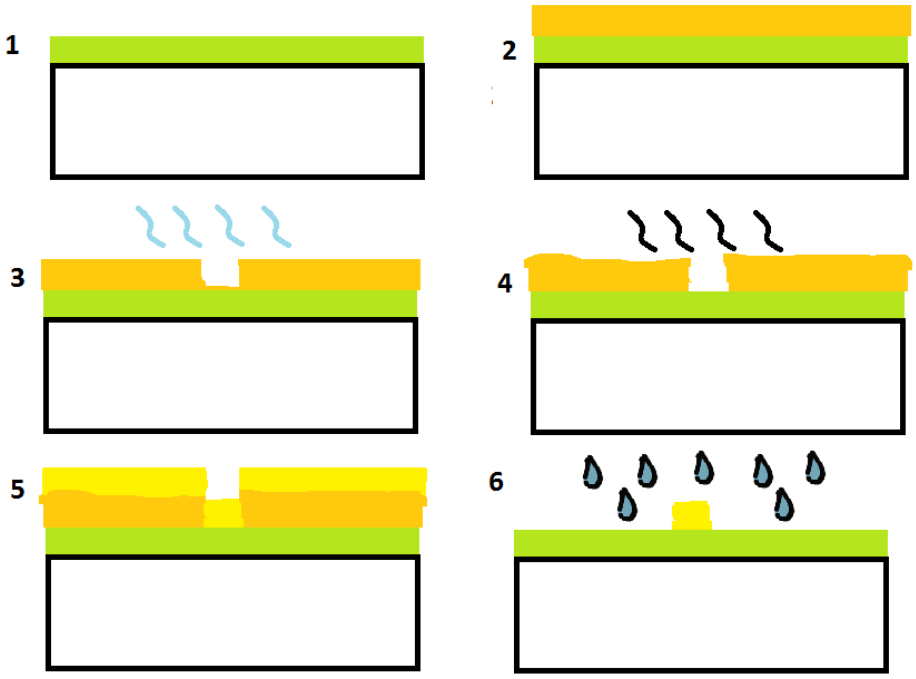

Figure 2.10. Draft of the steps for the nanoantenna fabrication.

Scanning electron microscope (SEM) pictures of the final result are shown:

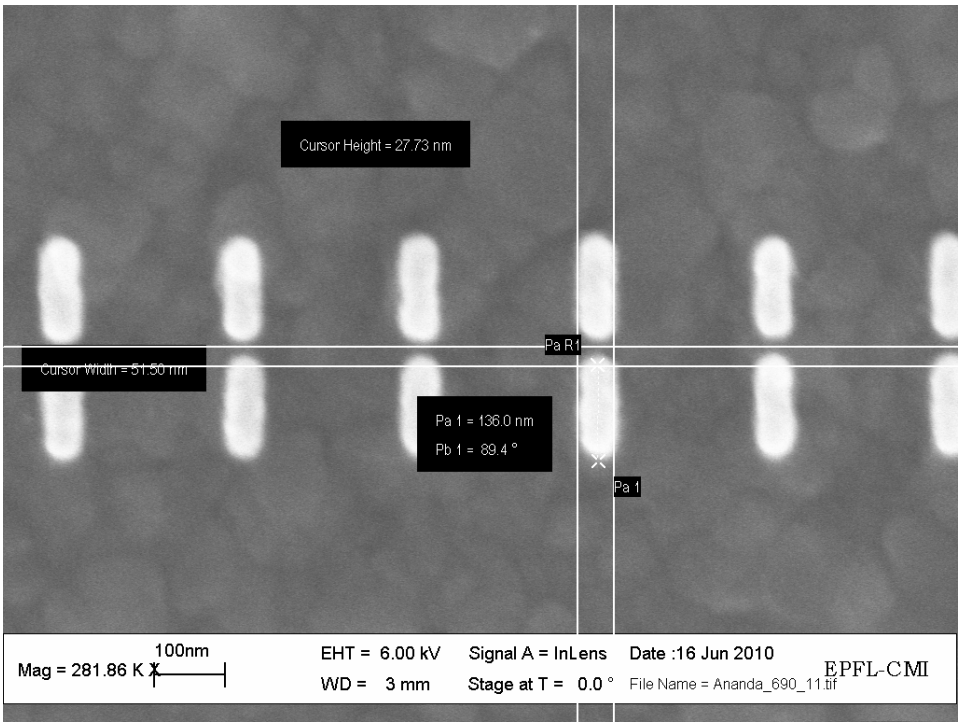

Figure 2.11 SEM picture of the nanoantennae. Dimension taken were (51.50nm width, 136nm length and 27.73nm gap)

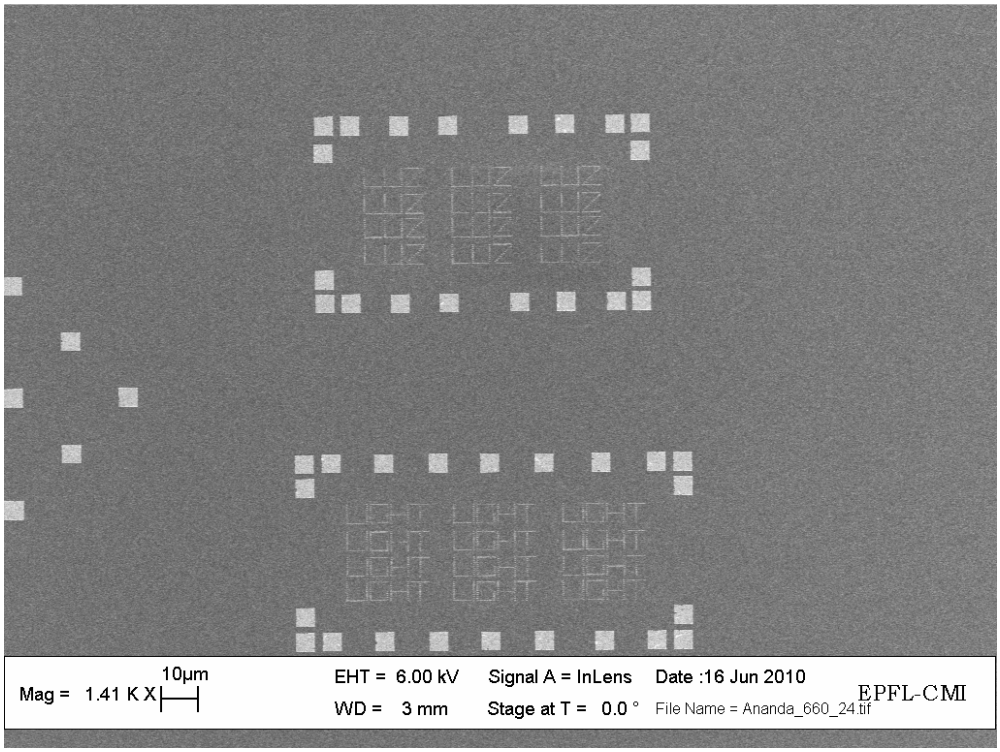

Figure 2.12 SEM picture of the mask of the nanoantennae.

From figure 2.11 we can see that the nanoantennae are wider than expected. We could confirm this with other images also taken at the SEM. Nevertheless we continue with the sample as it was for the measurement.

Figure 2.12 shows the mask used for the nanoantennae, here the squares are 5µm squares of gold used as markers in order to find easily the sample.

NANOANTENNA TESTING SETUP.

For testing our nanoantennae we used the setup shown in figure 2.13. Here the power and temperature of the Laser was controlled with a LASER DIODE COMBI CONTROLLER (ITC 510) from THORLABS. The laser wavelength is 1.55µm. Its output is guided towards a polarizer where we can select the polarization for checking if the light that we are seeing is actually the light coming from the nanoantennae. The output of the polarizer is guided to the output of the optical fiber hold by z,θ positioner for the posterior alignment of the fiber with the objectives. The objectives magnification are (from left to right) 10x, 100x and 40x. The first objective is used to receive the divergent light from the optical fiber and direct it into the second objective. Then the second objective is going to refocus the light into a smaller spot with a total demagnification of 10x. By doing this, we reduce the original spot coming from the fiber in order to have a diffraction limited spot which then is going to couple into the sample. The sample is hold in a x,y,z positioner, where we can move our sample few µm for coupling the light from the lens. After the sample there is our third objective positioned also in a x,y,z positioner. This objective is used for receiving the signal from the other side of the sample, so we can check the coupling in the waveguide. After the objective we see a prism. This prism is used for reflect the light coming from the objective towards the infrared camera

which is in the top of the setup (it is not shown in figure 2.13). The infrared camera will also be used for checking the radiation of the nanoantennae on top of the sample after having check that the light was couple into the waveguide. The optical fiber used was a single mode optical fiber with a mode field diameter around 10μm.

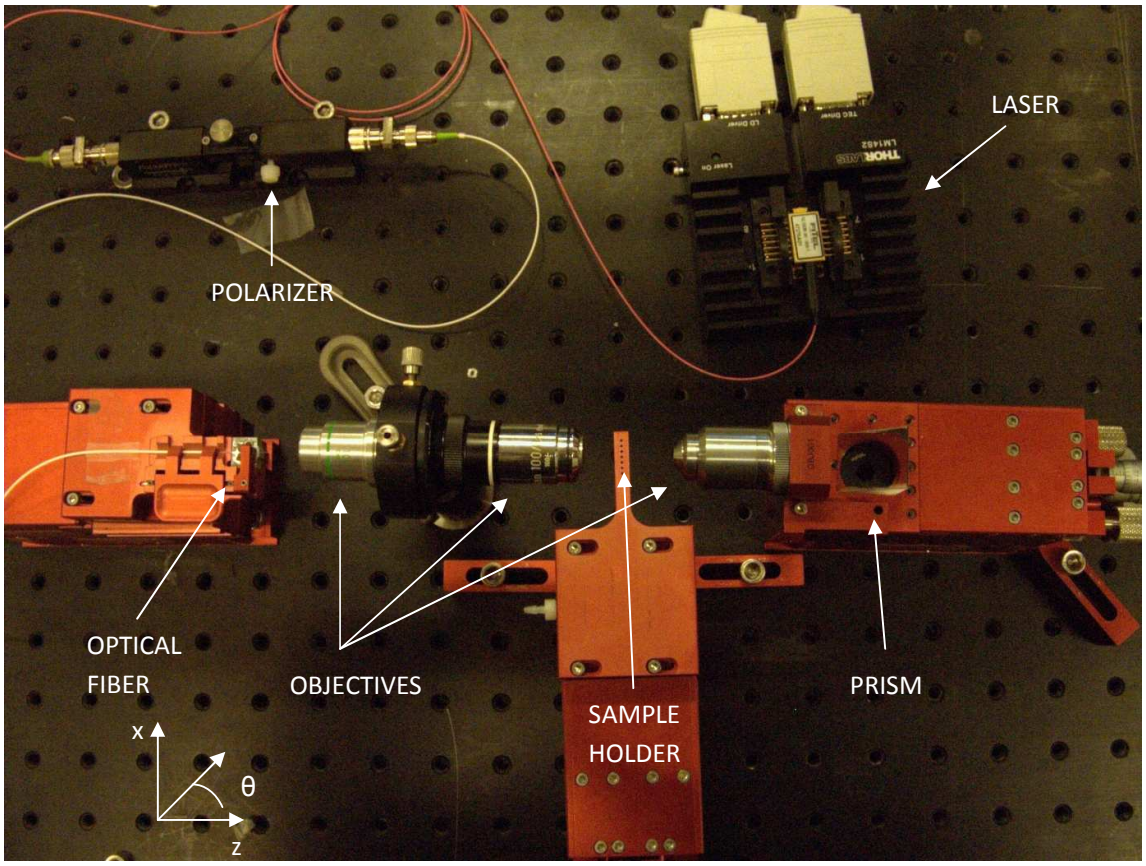

Figure 2.13. Experimental setup used for the testing of the nanoantenna

RESULTS AND ANALYSIS.

Problems

One big problem that we have to deal with was to couple the light on such a thin waveguide. In fact even if the spot coming out of the lens was nearly in the diffraction limit (around 1μm of field diameter) still it was not enough to couple all the light in the waveguide. The first substrate used for the deposition of the nanoantennae was as we said before a silicon substrate with a 500nm layer of silicon oxide. This substrate was chosen because the 500nm layer of silicon oxide was enough for separating the waveguide field from the substrate and because it was quite cheap. Nevertheless our light was even bigger than the sum of both waveguide and silicon oxide layers. Therefore we thought there was a lot of reflection in the silicon-silicon oxide layer and we changed our substrate for an entire silicon oxide substrate. Unfortunately during the fabrication of the nanoantennae in the silicon oxide substrate we forgot to realize the 4th step (Figure 2.10) and at the end we didn't get any nanoantenna.

Nevertheless we manage to couple light in our first sample even with some light going into the substrate; Figure 2.14 shows the image at the output of the 40x objective. But this light

going into the substrate will illuminate some dust and gold particles in our sample. This light coming from the scattering of those particles will also be received by the camera making difficult to distinguish between them and the nanoantennae. Still we try to look for the nanoantennae because it is supposed that their scattering field is very large. Therefore we look for them by shifting the polarization and looking for some spots which will stop shining when shifting the polarization, but we don't have any luck.

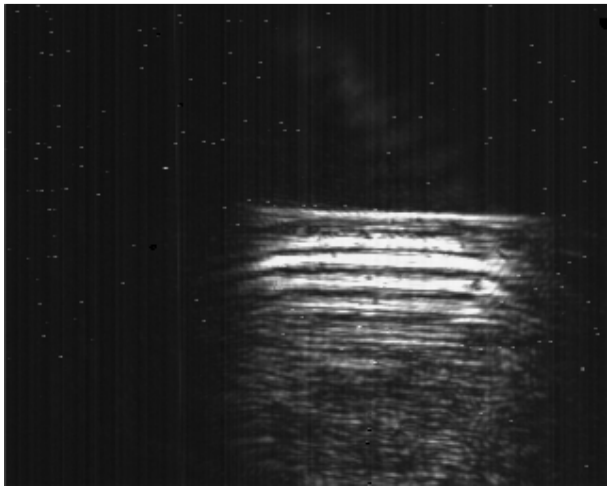

Figure 2.14. Image taken at the output of the 40x objective. Notice the high power in the top layer which shows the coupled light. The interference fringes are thought to be caused by the interference of the wave coming from the top layer.

We check also the silicon oxide substrate, because even without nanoantennae we could check if there were an increase in the light going into the waveguide as we believe, but in fact the light at the output had almost the same profile as in the case of the first substrate. So we thought it wasn't worth it to repeat the process again for this substrate.

Later we realize that another problem was the very small spot that we were focusing. In fact even if coupled in the waveguide, this spot while propagating into the waveguide will not diverge so much (around 5 or 10μm). Therefore the nanoantennae that we are trying to detect were in a line of around 5μm wider. This means that even if there were glowing nanoantennae, there were in a 5μm line which was very difficult to see with our camera which had only a 4x objective tube.

Also another important problem was the tilting of our sample. In fact if the sample is a little tilt in the xz plane (figure 2.13), the electric field exciting the nanoantennae will arrive in the wrong direction and may not excite the resonance frequency of the nanoantennae.

We can also attribute another problem from the fact that after the fabrication the nanoantennae were wider and bigger than expected and so they may have a shift in their resonance frequency and may not be excited in our wavelength.

Solutions.

From the previous section we can conclude that there are a lot of problems which can prevent the glowing of the nanoantennae. In fact I think that the substrate used for the excitation of the nanoantennae must be designed in order to guide the electric field towards the nanoantennae in the best way, in order to enhance as much as possible the response of the nanoantennae. This is not the case for our substrate.

Also a good design of the nanoantenna according to the results given in the fabrication has to be realized in order to have the dimensions that we want to.

In order to solve the problem of the substrate I propose a design of a waveguide as shown in figure 2.15. In this design the light coming from the lens is going to couple into this waveguide. The height and width of the waveguide can be very large (around 3 or 4 μm) allowing a diffractive limited spot to be guided in the waveguide without losses. This waveguide will guide the light towards the 400nm film of silicon, exciting the nanoantennae on top of it. In this design we see that the electric field is forced to arrive parallel to the nanoantennae as we want to, due to the waveguide boundary conditions. Still some simulations are needed in order to compute the losses due to the silicon oxide step. In fact there would be some light coming out in this silicon oxide step towards the substrate illuminating the little particles of gold and dust.

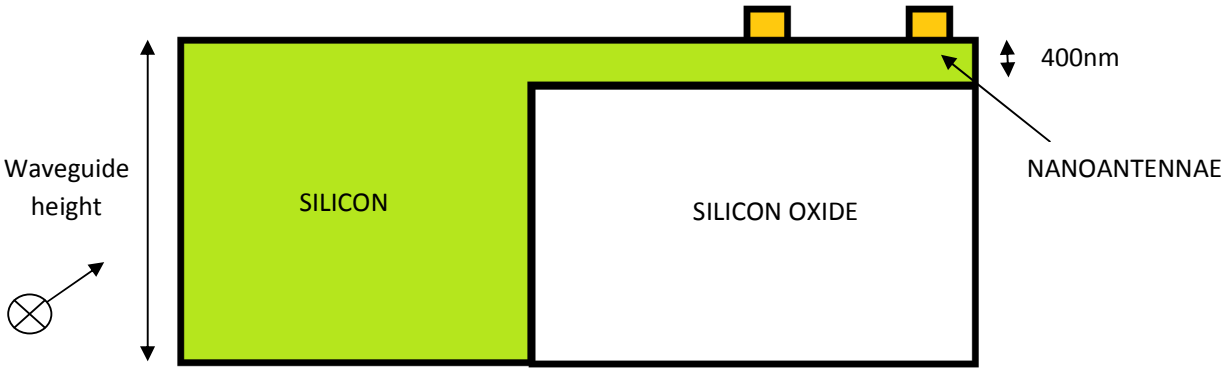

Figure 2.15. New design for the substrate employed for the nanoantennae test

Nevertheless there would be a large amount of power transmitted in the 400nm waveguide due to the coupling between the larger waveguide and the smaller waveguide, and we always can deposit a lot of nanoantennae in top of the silicon oxide along the waveguide in order to have a larger response with respect to the little particles and find the nanoantennae very easily with the camera. (in this case we will see a glowing line).

CONCLUSION

Plasmon waveguide:

- We find out that DLSPPW is the waveguide with fewer losses at small curvature radius; nevertheless this waveguide has more losses in comparison with other waveguides at larger curvature radius.
- In the case of the rectangular waveguides we saw that there is an optimum metal thickness which lower the losses according to the bending radius, this behavior can be understood as a consequence of the confinement dependence in the metal thickness.

Nanoantenna:

- Due to some problems in the experimental setup, the measurement of the nanoantennae radiation was not accomplished.
- A new design for the excitation of the nanoantennae has been proposed. This designed will overcome all the problems obtain in the experimental setup and will make the measurement possible.
- A change in the dimensions used in the mask for the fabrication of the nanoantennae has to be done in order to obtain the right dimensions after the fabrication.
- Simulations and a process flow for the fabrication of the new design have to be realized.

BIBLIOGRAPHY

1. Ozbay, E. (2006), 'Plasmonics: Merging Photonics and Electronics at Nanoscale Dimensions', *Science* **311**(5758), 189--193.

2. A. Fulbert and T. Pearsall, "A European roadmap for photonics and nanotechnology," MONA, Merging Optics & Nanotechnologies (2008)
.

3. S. K¨uhn, S. U. H°akanson, L. Rogobete, and V. Sandoghdar, “Enhancement of single-molecule fluorescence using a gold nanoparticle as an optical nanoantenna,” *Phys. Rev. Lett*. **97**, 017402 (2006).

4. Rich, R.L.; Myszka, D.G. Survey of the year 2006 commercial optical biosensor literature. *J. Mol.Recognit.* **2007**, *20*, 300-366.

5. Pillai, S.; Catchpole, K. R.; Trupke, T. & Green, M. A. (2007), 'Surface plasmon enhanced silicon solar cells', *Journal of Applied Physics* **101**(9), 093105+.

6. Degiron, A.; Dellagiacoma, C.; McIlhargey, J. G.; Shvets, G.; Martin, O. J. F. & Smith, D. R. (2007), 'Simulations of hybrid long-range plasmon modes with application to 90 bends', *Opt. Lett.* **32**(16), 2354--2356.

7. Dintinger, J. & Martin, O. J. F. (2009), 'Channel and wedge plasmon modes of metallic V-grooves with finite metal thickness', *Opt. Express* **17**(4), 2364--2374.

8. Holmgaard, T. & Bozhevolnyi, S. I. (2007), 'Theoretical analysis of dielectric-loaded surface plasmon-polariton waveguides', *Physical Review B (Condensed Matter and Materials Physics)* **75**(24), 245405+.

9. Moreno, E.; Garcia-Vidal, F. J.; Rodrigo, S. G.; Martin-Moreno, L. & Bozhevolnyi, S. I. (2006), 'Channel plasmon-polaritons: modal shape, dispersion, and losses', *Opt. Lett.* **31**(23), 3447--3449.

10. Maier, S. A. (2007), *Plasmonics: Fundamentals and Applications*, Springer, Berlin,

11. Johnson, P. B. & Christy, R. W. (1972), 'Optical Constants of the Noble Metals', *Phys. Rev. B* **6**(12), 4370--4379.

12. COMSOL Multiphysics version 3.5

13. Tsuji, Y. & Koshiba, M. (2002), 'Finite Element Method Using Port Truncation by Perfectly Matched Layer Boundary Conditions for Optical Waveguide Discontinuity Problems', *J. Lightwave Technol.* **20**(3), 463.

14. Teixeira, F. & Chew, W. (1997), 'Systematic derivation of anisotropic PML absorbing media in cylindrical and spherical coordinates', *Microwave and Guided Wave Letters, IEEE* **7**(11), 371 -373.

15. Chew, W.; Jin, J. & Michielssen, E. (1997), Complex coordinate system as a generalized absorbing boundary condition, *in* 'Antennas and Propagation Society International Symposium, 1997. IEEE., 1997 Digest', pp. 2060 -2063 vol.3.

16. Heng, X.; Cui, X.; Knapp, D. W.; Wu, J.; Yaqoob, Z.; McDowell, E. J.; Psaltis, D. & Yang,

C. (2006), 'Characterization of light collection through a subwavelength aperture from a point source', *Opt. Express* **14**(22), 10410--10425.

17. Holmgaard, T.; Chen, Z.; Bozhevolnyi, S. I.; Markey, L.; Dereux, A.; Krasavin, A. V. & Zayats, A. V. (2008), 'Bend- and splitting loss of dielectric-loaded surface plasmon-polariton waveguides', *Opt. Express* **16**(18), 13585--13592.

18. Fischer, H. & Martin, O. J. F. (2008), 'Engineering the optical response of plasmonic nanoantennae', *Opt. Express* **16**(12), 9144--9154.

19. Muhlschlegel, P.; Eisler, H.-J.; Martin, O. J. F.; Hecht, B. & Pohl, D. W. (2005), 'Resonant Optical Antennas', *Science* **308**(5728), 1607-1609.

20. Martin, O. J. F. & Piller, N. B. (1998), 'Electromagnetic scattering in polarizable backgrounds', *Phys. Rev. E* **58**(3), 3909--3915.

21. Fuchs, R. (1975), 'Theory of the optical properties of ionic crystal cubes', *Phys. Rev. B* **11**(4), 1732--1740.

ANNEX 1

Code employed for scat3d

Make3dGeom.param:

```
(1.d0,0.d0)          background
2                    nr. of objects
c                    cube
-20. -145. 0.        x0, y0, z0
10. 10. 10.          dx, dy, dz (mesh size)
4 13 4               nx, ny, nz (nr. of meshes)
11                   material (11=gold)
c                    cube
-20. 15. 0.          x0, y0, z0
10. 10. 10.          dx, dy, dz (mesh size)
4 13 4               nx, ny, nz (nr. of meshes)
11                   material (11=gold)
```

Scat3d.fld:

```
1
r                    reflex
-120.d0 0.d0         theta, phi
90.d0                polarization (s-polarization)

r                    reflex
-110.d0 0.d0         theta, phi
0.d0                 polarization (p-polarization
```

Scat3d.param:

```
Dipole antenna on Si substrate
1300.d0 1800.d0 11
1
(1.0d0,0.d0)         air
3                    Green's tensor type
(12.11d0,0.d0)             Silicon
```

Code employed for scatly3d

Make3dGeom.param:

```
(1.d0,0.d0)          background
2                    nr. of objects
c                    cube
-20. -145. 0.        x0, y0, z0
10. 10. 10.          dx, dy, dz (mesh size)
4 13 4               nx, ny, nz (nr. of meshes)
11                   material (11=gold)
c                    cube
-20. 15. 0.          x0, y0, z0
10. 10. 10.          dx, dy, dz (mesh size)
4 13 4               nx, ny, nz (nr. of meshes)
11                   material (11=gold)
```

Scat3d.fld:

```
1                    nr_excitations
m                    modal excitation
te                   polarization (tm: perp to plane of propagation,
0                    mode number (TAKE CARE OF NUMBERING)
0.d0                 propagation angle in xy-plane
```

Scat3d.param:

```
Dipole antenna on Si waveguide
1300.0d0 1700.0d0 5
2                    nr. interfaces
1                    material type (dielectric)
(1.d0,0.d0)          epsilon
(1.d0,0.d0)          mu
0.d0                 z-interface
1                    material type (dielectric Si)
(12.1106d0,0.d0)          epsilon
(1.d0,0.d0)          mu
-400.d0                   z-interface
1                    material type (dielectric SiO2)
(2.19d0,0.d0)        epsilon
(1.d0,0.d0)          mu
1                    type of Green's tensor (must be 1)
1                    integration (1=J or H), (2=J only)
```